

A Multifunctional Organic–Inorganic Hybrid Structure Based on Mn^{III}–Porphyrin and Polyoxometalate as a Highly Effective Dye Scavenger and Heterogeneous Catalyst

Chao Zou,[†] Zhijuan Zhang,[‡] Xuan Xu,[†] Qihan Gong,[‡] Jing Li,^{*,‡} and Chuan-De Wu^{*,‡}

[†]Department of Chemistry, Zhejiang University, Hangzhou 310027, P. R. China

[‡]Department of Chemistry and Chemical Biology, Rutgers University, Piscataway, New Jersey 08854-8087, United States

S Supporting Information

ABSTRACT: A two-step synthesis strategy has led to a unique layered polyoxometalate–Mn^{III}–metalloporphyrin-based hybrid material. The hybrid solid demonstrates remarkable capability for scavenging of dyes and for heterogeneous selective oxidation of alkylbenzenes with excellent product yields and 100% selectivity.

Crystalline organic–inorganic hybrids are a class of materials that integrate organic struts, inorganic clusters, and metal nodes in a framework structure. By incorporation of choice functional organic moieties and metal oxide clusters via self-assembly, grafting, or intercalation, such hybrid structures are formed with multiple functionalities and often new features as a result of blending of distinctively different components.¹ Within the context of nanostructured solids, complex hybrid systems provide a new pathway for combining multiple functional groups in a multilevel hierarchical framework at the molecular scale,² which demonstrates great potential for applications in diverse fields such as selective adsorption, catalysis, explosives detection, optics, optoelectronics, and electrochemicals.^{3–7}

Polyoxometalates (POMs) are a unique class of discrete anionic metal–oxygen clusters. POMs have attracted significant contemporary interest because of their unique functionality, making them active constituents in various materials.^{8–11} Particularly, the combination of POMs in hybrid networks can improve interactions between the organic molecules and the surface of metal oxides for efficient catalytic applications.¹²

Metalloporphyrins, which have unique biological, chemical, physical, and catalytic functionalities, represent a remarkable class of molecule-based solids.^{13,14} Because of their distinctive catalytic activities,¹⁵ the inclusion of metalloporphyrins in porous coordination networks has gained intense attention, and some of them have shown very interesting catalytic properties in heterogeneous reactions.^{14,16}

It is without question that the combination of POMs and metalloporphyrins in a porous hybrid material will not only retain the individual functionality but also introduce new and unique properties. However, the adverse solubility of these two moieties makes the synthesis of metalloporphyrin–POM-based hybrids extremely difficult.¹⁷

To meet such a challenge, we have developed a new synthetic method that has proved to be very efficient in

combining these two components in a hybrid structure. Herein we report the synthesis and characterization of the intercalated metalloporphyrin–POM-based hybrid framework $\{[\text{Cd}(\text{DMF})_2\text{Mn}^{\text{III}}(\text{DMF})_2\text{TPyP}](\text{PW}_{12}\text{O}_{40})\} \cdot 2\text{DMF} \cdot 5\text{H}_2\text{O}$ (**1**) (DMF = *N,N*-dimethylformamide; TPyP = tetrapyrrolylporphyrin), which demonstrates excellent capability for scavenging of dyes and for highly selective oxidation of alkylbenzenes.

To resolve the solubility issue of POMs (soluble in water) and porphyrins (soluble in organic solvents) under moderate reaction conditions, a reaction of $\text{H}_3\text{PW}_{12}\text{O}_{40}$ with $\text{Mn}^{\text{III}}\text{Cl}-\text{TPyP}$ in DMF was first carried out to form the zwitterionic complex $\{[\text{Mn}^{\text{III}}(\text{DMF})_2\text{TPyP}](\text{PW}_{12}\text{O}_{40})\}^{2-}$. The combined components could subsequently be dissolved effectively both in water and organic solvents (e.g., DMF, MeOH, etc.). By this strategy, we successfully isolated brownish crystals of **1** upon reaction of a mixture of the zwitterionic complex and $\text{Cd}(\text{NO}_3)_2 \cdot 4\text{H}_2\text{O}$ in a mixed solvent of DMF and acetic acid at 80 °C for 48 h.¹⁸

Single-crystal X-ray diffraction (XRD) analysis revealed that **1** crystallizes in the monoclinic *C2/c* space group and that its structure is built on alternate layers of POM anions and porphyrin-containing cationic nets.¹⁹ Each Cd^{II} ion octahedrally coordinates to the four pyridine groups of four TPyP ligands [$\text{Cd}-\text{N} = 2.34(1)-2.36(1)$ Å] at the equatorial positions and two DMF molecules [$\text{Cd}-\text{O} = 2.27(1)$ Å] at the apical sites. Each TPyP acts as a tetradentate ligand bridging four Cd^{II} ions to propagate a two-dimensional lamellar network of $[\text{Cd}(\text{DMF})_2\text{Mn}^{\text{III}}(\text{DMF})_2\text{TPyP}]_n^{3n+}$ parallel to the *ab* plane (Figure 1a). The Mn^{III} ion adopts a coplanar conformation with the porphyrin unit and coordinates to the four pyrroles of the porphyrin core [$\text{Mn}-\text{N} = 1.99(1)-2.03(1)$ Å] and two DMF molecules [$\text{Mn}-\text{O} = 2.21(1)$ Å] in an octahedral geometry. The lamellar 2D nets of $[\text{Cd}(\text{DMF})_2\text{Mn}^{\text{III}}(\text{DMF})_2\text{TPyP}]_n^{3n+}$ are packed in an ...AA... stacking sequence with a layer separation of 12.437(1) Å. The $[\text{PW}_{12}\text{O}_{40}]^{3-}$ polyanions are located between the lamellar networks [Figure 1 and Figure S1 in the Supporting Information (SI)]. It is interesting to note that only one of the two cavities between the lamellae is occupied by a $[\text{PW}_{12}\text{O}_{40}]^{3-}$ polyanion, while the other one is vacant to accommodate solvent molecules. As a result, compound **1** becomes porous upon solvent removal, with large cavities with dimensions of 10.07(1) Å × 10.09(1) Å ×

Received: September 29, 2011

Published: December 9, 2011

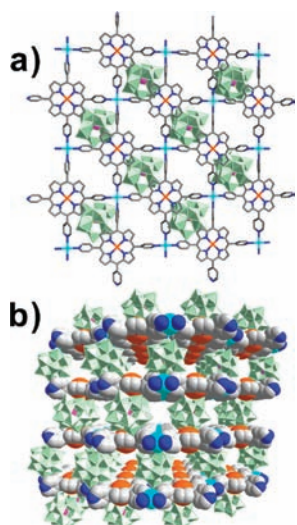


Figure 1. (a) Arrangement of a single layer of the lamellar framework of $[\text{Cd}(\text{DMF})_2\text{Mn}^{\text{III}}(\text{DMF})_2\text{TPyP}]_n^{3n+}$ and a layer of the $[\text{PW}_{12}\text{O}_{40}]^{3-}$ polyanions, as viewed down the c axis. (b) Perspective view of the packing diagram of **1** along the $[110]$ direction. Color scheme: Mn^{III} , orange; Cd, cyan; $\{\text{WO}_6\}$, green octahedra; P, purple; N, blue; C, gray. DMF molecules and H atoms have been omitted for clarity.

12.44(1) Å and 1D channel openings with dimensions of 5.36(1) Å \times 12.44(1) Å as viewed along the $[110]$ direction. PLATON calculations indicated that **1** contains 27.6% void space (2756.4 Å³ per unit cell) that is accessible to solvent molecules.²⁰ Thermogravimetric analysis showed that a weight loss of 5.5 wt % occurred between 25 and 164 °C, corresponding to the loss of guest DMF and H₂O molecules (calcd 5.5%). The release of DMF ligands occurred in the 164–241 °C region (calcd, 6.7%; found, 6.7%). No further weight loss was observed until 509 °C, above which **1** began to lose porphyrin ligand and framework decomposition occurred. When a sample of **1** was heated under vacuum at 100 °C for 12 h, ¹H NMR spectroscopy indicated that the lattice DMF molecules were almost fully evaporated (Figure S6b). Powder XRD (PXRD) analysis of the sample showed a sharp diffraction pattern identical to that of the pristine sample, indicating that the porous framework was maintained after the removal of solvent molecules.

Because of their complex structures and poor biodegradability, decolorization of widely used dyes is very difficult.²¹ Thus, scavenging such dyes from polluted water remains a challenging task. As compound **1** consists of two types of active components in its network structure, we used this material to remove dyes from aqueous solutions. When samples of **1** were added to aqueous solutions of methylene blue, rhodamine B, and crystal violet at room temperature, the dyes were almost fully adsorbed from their water solutions by solid **1**, as monitored by UV–vis absorption spectroscopy (Figure 2a–c). As shown in Figure 2d, 1 g of solid **1** can adsorb 0.033 mmol of methylene blue, 0.063 mmol of rhodamine B, and 0.057 mmol of crystal violet. A comparison of the amounts of adsorbed dye indicates that **1** has significantly higher capture capability than either MnCl–TPyP or $[\text{Bu}_4\text{N}]_3[\text{PW}_{12}\text{O}_{40}]$ (Figure 2d).

To identify the adsorption sites of the dye molecules (e.g., on the solid surfaces or in the open channels), we immersed a sample of **1** in an aqueous solution of methylene blue at 50 °C for 24 h. After this treatment, the crystals of **1** showed no apparent difference in comparison to the original form except

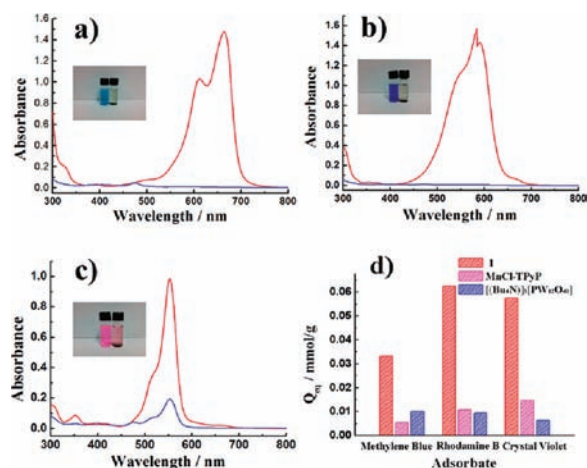
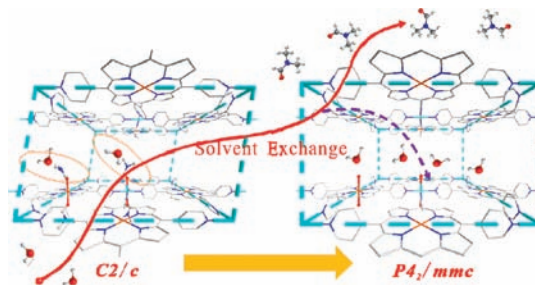


Figure 2. (a–c) UV–vis spectra of (a) methylene blue, (b) crystal violet, and (c) rhodamine B before (red lines) and after (blue lines) the addition of solid **1**. The inset photographs highlight the scavenging effects. (left) before scavenging; (right) after scavenging. (d) Comparison of the dye capture capacities of **1** (red), the MnCl–TPyP ligand (pink), and $[\text{Bu}_4\text{N}]_3[\text{PW}_{12}\text{O}_{40}]$ (blue).

for a slightly deepened color. However, the PXRD pattern of the treated sample showed significant changes. Single-crystal XRD analysis revealed that the resultant compound $\{[\text{Cd}(\text{H}_2\text{O})_2\text{Mn}^{\text{III}}(\text{H}_2\text{O})_2\text{TPyP}](\text{PW}_{12}\text{O}_{40})\} \cdot 10\text{H}_2\text{O}$ (**2**) was very similar to **1**, except that the DMF ligands were replaced by water molecules (Scheme 1).¹⁹ The space group of **2** is

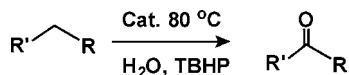
Scheme 1. Schematic Representation of the Single-Crystal to Single-Crystal Transformation from **1** to **2** Induced by Ligated Solvent Exchange (See Figure S2 and Table S3 for Details)

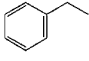
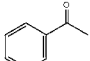
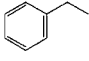
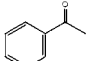
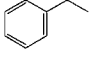
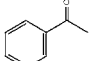
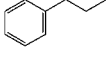
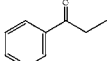
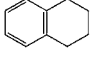
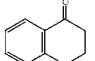
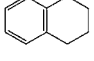
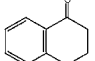
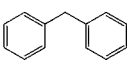
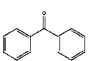
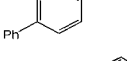
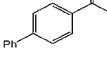
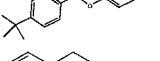
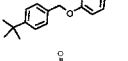
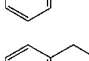
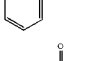
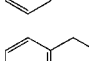
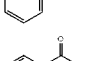
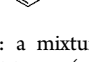
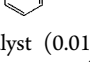


tetragonal $P4_1/mmc$ as opposed to monoclinic $C2/c$ for **1**. The single-crystal to single-crystal (SC–SC) transformation is accompanied by a reduction of the c axis length from 24.8738(8) to 23.636(4) Å and large variations in the angles. Combining this observation with the captured amounts of the dyes, it can be concluded that the adsorption of the dyes occurs on the solid surfaces.

As **1** contains catalytically active Mn^{III} –TPyP species and its backbone remains intact after the substitution of the ligated DMF by water molecules, we were encouraged to evaluate the catalytic ability of **1** in the oxidation reaction of alkylbenzene. Oxidation of ethylbenzene (EB) by **1** was conveniently performed in H₂O at 80 °C for 12 h using *tert*-butylhydroperoxide (TBHP) as the oxidant (see Scheme 2). GC–MS analysis showed that only one product, acetophenone, was formed in an excellent yield of 92.7% (Table 1, entry 1). For comparison, a series of control catalysts were also

Scheme 2. Oxidation Reaction of Alkylbenzenes

Table 1. Selective Oxidation of Alkylbenzenes for the Formation of Phenyl Ketones^a

Entry	Substrate	Product	Catalyst	Yd,% ^b
1			1	92.7
2			MnCl-TPyP	73.6
3			H ₃ PW ₁₂ O ₄₀	0
4			1	92.0
5			1	82.2
6			MnCl-TPyP	55.3
7			1	37.0
8			1	25.6
9			1	19.5
10			1	90.4 ^c
11			1	85.4 ^d
12			MnCl-TPyP	2.6 ^c

^aConditions: a mixture of catalyst (0.01 mmol), alkylbenzene (0.1 mmol), and TBHP (0.5 mmol) in water (5 mL) was stirred at 80 °C for 12 h. ^bBased on GC analysis. ^cThe second cycle. ^dThe sixth cycle.

employed in the same catalytic experiments. Mn^{III}Cl-TPyP was considerably less efficient, with a 73.6% yield for acetophenone, while [PW₁₂O₄₀]³⁻ showed no activity (Table 1, entries 2 and 3). These results suggest that the catalytic activity of **1** is superior to those of its precursors. Under the same catalytic conditions, catalyst **1** can also oxidize propylbenzene and tetrahydronaphthalene, giving rise to the corresponding ketones in excellent yields with 100% selectivity (Table 1, entries 4 and 5). Much lower yields were obtained in the cases of larger substrate molecules, most likely because the reactions occur only on the solid surfaces (Table 1, entries 7–9).

After a mixture of solid **1** and TBHP in H₂O was heated at 80 °C for 12 h under stirring, EB and additional TBHP were subsequently added into the hot filtrate, which was heated at 80 °C for another 12 h. GC analysis indicated that the mixture was unreactive. This experiment proved that the hybrid catalyst system is heterogeneous in nature. Solid **1** was easily recovered

by filtration and subsequently used in successive runs with only slightly decreased product yields (Table 1, entries 10 and 11). On the contrary, the catalytic activity was greatly depressed when the recovered homogeneous Mn^{III}Cl-TPyP was used instead of solid **1** (Table 1, entry 12).

We monitored the accessibility of the open channels to several substrate molecules by ¹H NMR, GC-MS, and liquid-phase adsorption experiments (see the SI for details). The NMR spectrum is clearly indicative of pore accessibility to EB molecules. A more quantitative analysis was conducted by GC-MS and liquid-phase adsorption, from which uptake amounts of 13.2 and 15.2 wt % were obtained, respectively. On the contrary, no detectable amount was observed by either ¹H NMR or GC-MS analysis for larger substrate molecules such as 4-ethylbiphenyl and 1-(*tert*-butyl)-4-((4-ethylphenoxy)methyl)benzene under the same experimental conditions. Additionally, gas-phase CO₂ adsorption experiments were carried out on both samples of **1** and **2** in the vicinity of room temperature (0, 15, and 25 °C; see Figure S12) to evaluate the porosities of **1** and **2**. The estimated Langmuir and Brunauer-Emmett-Teller surface areas were 133 and 65 m²/g for **1** and 124 and 82 m²/g for **2**, respectively. These combined results suggest that the Mn^{III} sites in the channel walls are indeed reachable by substrates of relatively small sizes, thus allowing much higher catalytic performance than in the case of larger substrates. The latter molecules have difficulty entering the interior pore spaces, and reactions can only occur at exterior solid surfaces. It is interesting to note that after the reaction of **1** in a mixture of EB, H₂O, and TBHP at 80 °C for 24 h, the backbone of the resultant structure {[Cd(H₂O)₂Mn^{III}(H₂O)₂TPyP](PW₁₂O₄₀)} (**3**) was identical to that of **2**.¹⁹

It has been proposed that hydrocarbon oxidation catalyzed by metalloporphyrins involves the formation of reactive oxometalloporphyrin intermediates.²² However, a big disadvantage in homogeneous catalysis using metalloporphyrins is that suicidal inactivation is inevitable because of the formation of catalytically inactive μ -oxo metalloporphyrin dimers.²³ The remarkable stability of compound **1** should be attributed to the very robust layered framework of the Mn^{III}-porphyrin units separated by [PW₁₂O₄₀]³⁻ polyanions, which prevents the formation of inactivated dimers.

In summary, we have developed a new strategy for the effective synthesis of a novel POM-Mn^{III}-metalloporphyrin-based hybrid layered framework. Compound **1** combines multiple functional groups in a single structure. It exhibits remarkable capability for scavenging of dyes and heterogeneous selective oxidation of alkylbenzenes with high yields and 100% selectivity. Our results from catalytic reactions have also demonstrated excellent size selectivity of **1** in accordance with its pore dimensions. This work provides a new pathway for the future synthesis of POM-porphyrin hybrid materials with merged functionality for potential applications.

■ ASSOCIATED CONTENT

📄 Supporting Information

Experimental procedures, additional figures and tables, and crystallographic data. This material is available free of charge via the Internet at <http://pubs.acs.org>.

■ AUTHOR INFORMATION

Corresponding Author

jingli@rutgers.edu; cdwu@zju.edu.cn

ACKNOWLEDGMENTS

This work was financially supported by the NNSF of China (Grant 21073158), the Zhejiang Provincial Natural Science Foundation of China (Grant Z4100038), and the Fundamental Research Funds for the Central Universities (Grant 2010QNA3013). The RU team acknowledges partial support from DOE (Grant DE-FG02-08ER46491).

REFERENCES

- (1) (a) Férey, G.; Mellot-Draznieks, C.; Serre, C.; Millange, F. *Acc. Chem. Res.* **2005**, *38*, 217. (b) Rosseinsky, M. J. *Microporous Mesoporous Mater.* **2004**, *73*, 15. (c) MasPOCH, D.; Ruiz-Molina, D.; Veciana, J. *Chem. Soc. Rev.* **2007**, *36*, 770. (d) Rowsell, J. L. C.; Yaghi, O. M. *Microporous Mesoporous Mater.* **2004**, *73*, 3. (e) Cheetham, A. K.; Rao, C. N. R.; Feller, R. K. *Chem. Commun.* **2006**, 4780.
- (2) *Functional Hybrid Materials*; Gómez-Romero, P., Sanchez, C., Eds.; Wiley-VCH: Weinheim, Germany, 2004.
- (3) El-Nahal, Y.; Nir, S.; Serban, C.; Rabinovitch, O.; Rubin, B. J. *Agric. Food Chem.* **2000**, *48*, 4791.
- (4) *Chiral Catalysts Immobilization and Recycling*; De Vos, D. E., Vankelecom, I. F. J., Jacobs, P. A., Eds.; Wiley-VCH: Weinheim, Germany, 2000.
- (5) (a) Braun, I.; Ihlein, G.; Laeri, F.; Nöckel, J. U.; Schulz-Ekloff, G.; Schüth, F.; Vietze, U.; Weiß, Ö.; Wöhrle, D. *Appl. Phys. B: Lasers Opt.* **2000**, *70*, 335. (b) Ruiz-Hitzky, E. *J. Mater. Chem.* **2001**, *11*, 86.
- (6) (a) Wellmann, H.; Rathousky, J.; Wark, M.; Zukal, A.; Schulz-Ekloff, G. *Microporous Mesoporous Mater.* **2001**, *44*, 419. (b) Torres-Gómez, G.; Tejada-Rosales, E. M.; Gómez-Romero, P. *Chem. Mater.* **2001**, *13*, 3693.
- (7) (a) Lan, A. J.; Li, K. H.; Wu, H. H.; Olson, D. H.; Emge, T. J.; Ki, W.; Hong, M. C.; Li, J. *Angew. Chem. Intl. Ed.* **2009**, *48*, 2334. (b) Pramanik, S.; Zheng, C.; Emge, T. J.; Li, J. *J. Am. Chem. Soc.* **2011**, *133*, 4153.
- (8) (a) Hill, C. L. *Chem. Rev.* **1998**, *98*, 1. (b) Coronado, E.; Giménez-Saiz, C.; Gómez-García, C. J. *Coord. Chem. Rev.* **2005**, *249*, 1776. (c) Akutagawa, T.; Endo, D.; Noro, S.-I.; Cronin, L.; Nakamura, T. *Coord. Chem. Rev.* **2007**, *251*, 2547. (d) Yu, R.; Kuang, X.-F.; Wu, X.-Y.; Lu, C.-Z.; Donahue, J. P. *Coord. Chem. Rev.* **2009**, *253*, 2872. (e) Kortz, U.; Müller, A.; van Slageren, J.; Schnak, J.; Dalal, N. S.; Dressel, M. *Coord. Chem. Rev.* **2009**, *253*, 2315. (f) Long, D.-L.; Tsunashima, R.; Cronin, L. *Angew. Chem., Int. Ed.* **2010**, *49*, 1736.
- (9) Mizuno, N.; Yamaguchi, K.; Kamata, K. *Coord. Chem. Rev.* **2005**, *249*, 1944.
- (10) Keita, B.; Nadjó, L. In *Encyclopedia of Electrochemistry*; Bard, A. J., Stratmann, M., Eds.; Wiley-VCH: Weinheim, Germany, 2006.
- (11) Kögler, P.; Tsukerblat, B.; Müller, A. *Dalton Trans.* **2010**, 39, 21.
- (12) (a) Dolbecq, A.; Dumas, E.; Mayer, C. R.; Mialane, P. *Chem. Rev.* **2010**, *110*, 6009. (b) Song, J.; Luo, Z.; Britt, D. K.; Furukawa, H.; Yaghi, O. M.; Hardcastle, K. I.; Hill, C. L. *J. Am. Chem. Soc.* **2011**, *133*, 16839.
- (13) (a) Chang, J. W. W.; Chan, P. W. H. *Angew. Chem., Int. Ed.* **2008**, *47*, 1138. (b) Jiang, G.; Chen, J.; Thu, H.-Y.; Huang, J.-S.; Zhu, N.; Che, C.-M. *Angew. Chem., Int. Ed.* **2008**, *47*, 6638. (c) Li, C.-Y.; Wang, X.-B.; Sun, X.-L.; Tang, Y.; Zheng, J.-C.; Xu, Z.-H.; Zhou, Y.-G.; Dai, L.-X. *J. Am. Chem. Soc.* **2007**, *129*, 1494. (d) Simonneaux, G.; Le Maux, P.; Ferrand, Y.; Rault-Berthelot, J. *Coord. Chem. Rev.* **2006**, *250*, 2212. (e) *The Porphyrin Handbook*; Kadish, K. M., Smith, K. M., Guillard, R., Eds.; Academic Press: San Diego, 2000; (f) Lee, S. J.; Hupp, J. T. *Coord. Chem. Rev.* **2006**, *250*, 1710. (g) Lee, S. J.; Malliakas, C. D.; Kanatzidis, M. G.; Hupp, J. T.; Nguyen, S. T. *Adv. Mater.* **2008**, *20*, 3543. (h) Lee, S. J.; Cho, S.-H.; Mulfort, K. L.; Tiede, D. M.; Hupp, J. T.; Nguyen, S. T. *J. Am. Chem. Soc.* **2008**, *130*, 16828. (i) Hupp, J. T. *Nat. Chem.* **2010**, *2*, 432. (j) She, C.; Lee, S. J.; McGarrah, J. E.; Vura-Weis, J.; Wasielewski, M. R.; Chen, H.; Schatz, G. C.; Ratner, M. A.; Hupp, J. T. *Chem. Commun.* **2010**, 46, 547.
- (14) (a) Abrahams, B. F.; Hoskins, B. F.; Michall, D. M.; Robson, R. *Nature* **1994**, *369*, 727. (b) Byrn, M. P.; Curtis, C. J.; Hsiou, Y.; Khan, S. I.; Sawin, P. A.; Tendick, S. K.; Terzis, A.; Strouse, C. E. *J. Am. Chem. Soc.* **1993**, *115*, 9480. (c) Smithenry, D. W.; Wilson, S. R.; Suslick, K. S. *Inorg. Chem.* **2003**, *42*, 7719. (d) Goldberg, I. *Chem. Commun.* **2005**, 1243. (e) Bar, A. K.; Chakrabarty, R.; Mostafa, G.; Mukherjee, P. S. *Angew. Chem., Int. Ed.* **2008**, *47*, 8455. (f) Ohmura, T.; Usuki, A.; Fukumori, K.; Ohta, T.; Ito, M.; Tatsumi, K. *Inorg. Chem.* **2006**, *45*, 7988. (g) Choi, E.-Y.; Barron, P. M.; Novotny, R. W.; Son, H.-T.; Hu, C.; Choe, W. *Inorg. Chem.* **2009**, *48*, 426. (h) Deiters, E.; Bulach, V.; Hosseini, M. W. *Chem. Commun.* **2005**, 3906. (i) Pan, L.; Kelly, S.; Huang, X.; Li, J. *Chem. Commun.* **2002**, 2334. (j) Kosal, M. E.; Chou, J.-H.; Wilson, S. R.; Suslick, K. S. *Nat. Mater.* **2002**, *1*, 118.
- (15) (a) Collman, J. P.; Boulatov, R.; Sunderland, C. J.; Fu, L. *Chem. Rev.* **2003**, *104*, 561. (b) *Metalloporphyrins in Catalytic Oxidations*; Sheldon, R. A., Ed.; Marcel Dekker: New York, 1994. (c) Suslick, K. S.; Van Deusen-Jeffries, S. In *Comprehensive Supramolecular Chemistry: Bioinorganic Systems*; Suslick, K. S., Ed.; Elsevier: Oxford, U.K., 1996.
- (16) (a) Suslick, K. S.; Bhyrappa, P.; Chou, J.-H.; Kosal, M. E.; Nakagaki, S.; Smithenry, D. W.; Wilson, S. R. *Acc. Chem. Res.* **2005**, *38*, 283. (b) Shultz, A. M.; Farha, O. K.; Hupp, J. T.; Nguyen, S. T. *J. Am. Chem. Soc.* **2009**, *131*, 4204. (c) Shultz, A. M.; Farha, O. K.; Hupp, J. T.; Nguyen, S. T. *Chem. Sci.* **2011**, *2*, 686. (d) Farha, O. K.; Shultz, A. M.; Sarjeant, A. A.; Nguyen, S. T.; Hupp, J. T. *J. Am. Chem. Soc.* **2011**, *133*, 5652. (e) Xie, M.-H.; Yang, X.-L.; Zou, C.; Wu, C.-D. *Inorg. Chem.* **2011**, *50*, 5318. (f) Xie, M.-H.; Yang, X.-L.; Wu, C.-D. *Chem. Commun.* **2011**, 47, 5521.
- (17) Hagrman, D.; Hagrman, P. J.; Zubieta, J. *Angew. Chem., Int. Ed.* **1999**, *38*, 3165.
- (18) Yield: 51 mg. Anal. Calcd for **1** (%): C, 18.10; H, 1.90; N, 5.28. Found (%): C, 18.16; H, 1.88; N, 5.23. IR (KBr pellet) ν (cm⁻¹): 1648 (s), 1608 (m), 1544 (w), 1495 (w), 1436 (w), 1419 (w), 1384 (m), 1345 (w), 1252 (w), 1207 (w), 1079 (m), 1049 (w), 1011 (w), 978 (m), 951 (w), 896 (m), 822 (s), 714 (w), 595 (w), 564 (w), 521 (w).
- (19) Crystal data for **1**: C₆₄H₈₀CdMnN₁₆O₄₈PW₁₂, M_r = 4336.03; monoclinic, space group C2/c; a = 20.1333(8) Å, b = 20.1906(6) Å, c = 24.8738(8) Å, β = 98.952(4)°; V = 9988.1(6) Å³, Z = 4; D_{calcd} = 2.883 g·cm⁻³; μ = 14.202 mm⁻¹; F(000) = 7944, R₁ = 0.0660, wR₂ = 0.1567, S = 1.098. Crystal data for **2**: C₄₀H₃₂CdMnN₈O₄₄PW₁₂, M_r = 3733.25; tetragonal, space group P4₂/mmc; a = 14.1159(6) Å, c = 23.636(4) Å; V = 4709.7(9) Å³, Z = 2; D_{calcd} = 2.633 g·cm⁻³; μ = 15.028 mm⁻¹; F(000) = 3312, R₁ = 0.1050, wR₂ = 0.2143, S = 1.027. Crystal data for **3**: C₄₀H₃₂CdMnN₈O₄₄PW₁₂, M_r = 3733.25; tetragonal, space group P4₂/mmc; a = 14.1967(7) Å, c = 22.8003(18) Å; V = 4595.3(5) Å³, Z = 2; D_{calcd} = 2.698 g·cm⁻³; μ = 15.402 mm⁻¹; F(000) = 3312, R₁ = 0.1096, wR₂ = 0.2560; S = 1.280.
- (20) Spek, A. L. *PLATON: A Multipurpose Crystallographic Tool*; Utrecht University: Utrecht, The Netherlands, 2001.
- (21) (a) Al-Ghouti, M. A.; Khraisheh, M.; Allen, S. J.; Ahmad, M. N. *J. Environ. Manage.* **2003**, *69*, 229. (b) Zhou, L.; Gao, C.; Xu, W. *ACS Appl. Mater. Interfaces* **2010**, *2*, 1483.
- (22) (a) Zhang, J.-L.; Huang, J.-S.; Che, C.-M. *Chem.—Eur. J.* **2006**, *12*, 3020. (b) McLain, J. L.; Lee, J.; Groves, J. T. In *Biomimetic Oxidations Catalyzed by Transition Metal Complexes*; Meunier, B., Ed.; Imperial College Press: London, 2000.
- (23) (a) Walker, F. A.; Simonis, U. *Iron Porphyrin Chemistry*. In *Encyclopedia of Inorganic Chemistry*, 2nd ed.; Wiley: Chichester, U.K., 2006. (b) Merlau, M. L.; Borg-Breen, C. C.; Nguyen, S. T. *Epoxidation—Homogeneous*. In *Encyclopedia of Catalysis*; Wiley: New York, 2002.